Orbital Edelstein effect in topological insulators

Ken Osumi
Tokyo Institute of Technology
Tiantian Zhang
Tokyo Institute of Technology
Shuichi Murakami (murakami@stat.phys.titech.ac.jp)
Tokyo Institute of Technology https://orcid.org/0000-0002-2033-9402

Physics Article

Keywords: orbital Edelstein effect, topological insulators

Posted Date: February 1st, 2021

DOI: https://doi.org/10.21203/rs.3.rs-150034/v1

Version of Record: A version of this preprint was published at Communications Physics on September 21st, 2021. See the published version at https://doi.org/10.1038/s42005-021-00702-4.

Orbital Edelstein effect in topological insulators

Ken Osumi,[1] Tiantian Zhang,[1,2] and Shuichi Murakami[1,2,*]

[1] *Department of Physics, Tokyo Institute of Technology, Tokyo 152-8551, Japan*
[2] *TIES, Tokyo Institute of Technology, Tokyo 152-8551, Japan*

(Dated: today)

We theoretically propose a gigantic orbital Edelstein effect in topological insulators and interpret the results in terms of topological surface currents. We numerically calculate the orbital Edelstein effect for a model of a three-dimensional Chern insulator as an example. Furthermore, we calculate the orbital Edelstein effect as a surface quantity using a surface Hamiltonian of a topological insulator, and numerically show that it well describes the results by direct numerical calculation. We find that the orbital Edelstein effect depends on the local crystal structure of the surface, which shows that the orbital Edelstein effect cannot be defined as a bulk quantity. We propose that Chern insulators and Z_2 topological insulators can be a platform with a large orbital Edelstein effect because current flows only along the surface. We also propose candidate topological insulators for this effect. As a result, the orbital magnetization as a response to the current is much larger in topological insulators than that in metals by many orders of magnitude.

In recent years, new responses leading to orbital magnetization have been proposed in systems without inversion symmetry[1–16]. One of the focuses is conversion of electron current and magnetization on crystal structure with low symmetry. Among such proposals are orbital Edelstein effect (OEE)[1–3,10,11,13–15], i.e. current-induced orbital magnetization, and the gyrotropic effect[4–6]. These effects have similar response coefficients. In particular, OEE is an orbital analog of the Edelstein effect[17–19]. OEE emerges even in systems without spin-orbit interactions[1,3]. In particular, the OEE emerges in crystals with a chiral structure[1–3], similar to the phenomenon in which the solenoid creates a magnetic field when a current flows. As a similar context, the recent finding of spin-selective electron transport through chiral molecules, the so-called chirality-induced spin selectivity (CISS) effect[20–24], suggests an alternative method of using organic materials as spin filters for spintronics applications.

In the OEE, the electric field induces the magnetization, which may look similar to the magnetoelectric effect[25–33]. Nonetheless, in the spin and OEE, metallic systems are considered, and nonequilibrium electron distribution by the electric field is a key to generate magnetization. In this sense, the Edelstein effect can be called kinetic magnetoelectric effect. On the other hand, in the magnetoelectric effect, insulating systems are considered and the system stays in equilibrium even under the electric field or the magnetic field. Correspondingly, symmetry requirements are different. In the magnetoelectric effect, inversion and time-reversal symmetries should be broken but their product symmetry is preserved. On the other hand, in the Edelstein effect, the inversion symmetry should be broken. It is seen in chiral systems[1–3,10,11,13,14], and in polar systems[15].

Magnetoelectric tensors may require careful consideration of boundaries. While orbital magnetization is independent on the boundary[34–39], the orbital magnetization when an electric field is applied may not have such properties. The general orbital magnetoelectric response[30–33] depends on the boundary[37]. Therefore, it is important to study the effect of the boundary of the response of orbital magnetization.

In this paper, we investigate OEE in topological insulators such as three-dimensional Chern insulators and Z_2 topological insulators (Z_2-TIs)[40–42] in which the currents are localized on the surface. First, we calculate the OEE in three-dimensional topological insulators with chiral crystal structure. Second, we derive the OEE based on the surface Hamiltonian, and we show that this effect depends on surface states. Finally, we propose candidate materials for this effect and estimate the values of the OEE. By comparing the results with the results in a chiral semiconductor tellurium[5], we show that in topological insulators the orbital magnetization as a response to the current is much larger than metals by many orders of magnitude.

Results

Formulation for OEE. We consider a crystal in a shape of a cylinder along the z-axis, and calculate its orbital magnetization along the z-axis generated by the current along the z-axis. Let c be the lattice constant along the z-axis. We introduce the velocity operator $\mathbf{v}$ as $\mathbf{v} = -\frac{i}{\hbar}[\mathbf{r}, H]$, where $\mathbf{r}$ is the position operator and H is the Hamiltonian. In the limit of the system length along the z-axis to be infinity, the orbital magnetization at zero temperature is

$$M_z = \frac{1}{2\pi}\int_{-\pi/c}^{\pi/c} dk_z \frac{1}{S}\sum_n^N f(E_n(k_z)) \times \left(-\frac{e}{2}\right)\langle\psi_n(k_z)|(\mathbf{r}\times\mathbf{v})_z|\psi_n(k_z)\rangle, \qquad (1)$$

where $-e$ is the electron charge, $|\psi_n(k_z)\rangle$ and E_n are the nth occupied eigenstates and energy eigenvalues of H at the Bloch wavenumber k_z, respectively. $f(E)$ is the distribution function at the energy E, S is the cross section of the crystal along the xy-plane and N is the number of occupied states.

Then, within the Boltzman approximation, the applied electric field E_z changes $f(E)$ from $f^0(E)$ into $f(E) = f^0(E) + \frac{e\tau E_z}{\hbar}\frac{\partial f^0(E)}{\partial k_z}$ in a linear order in E_z, where τ is the

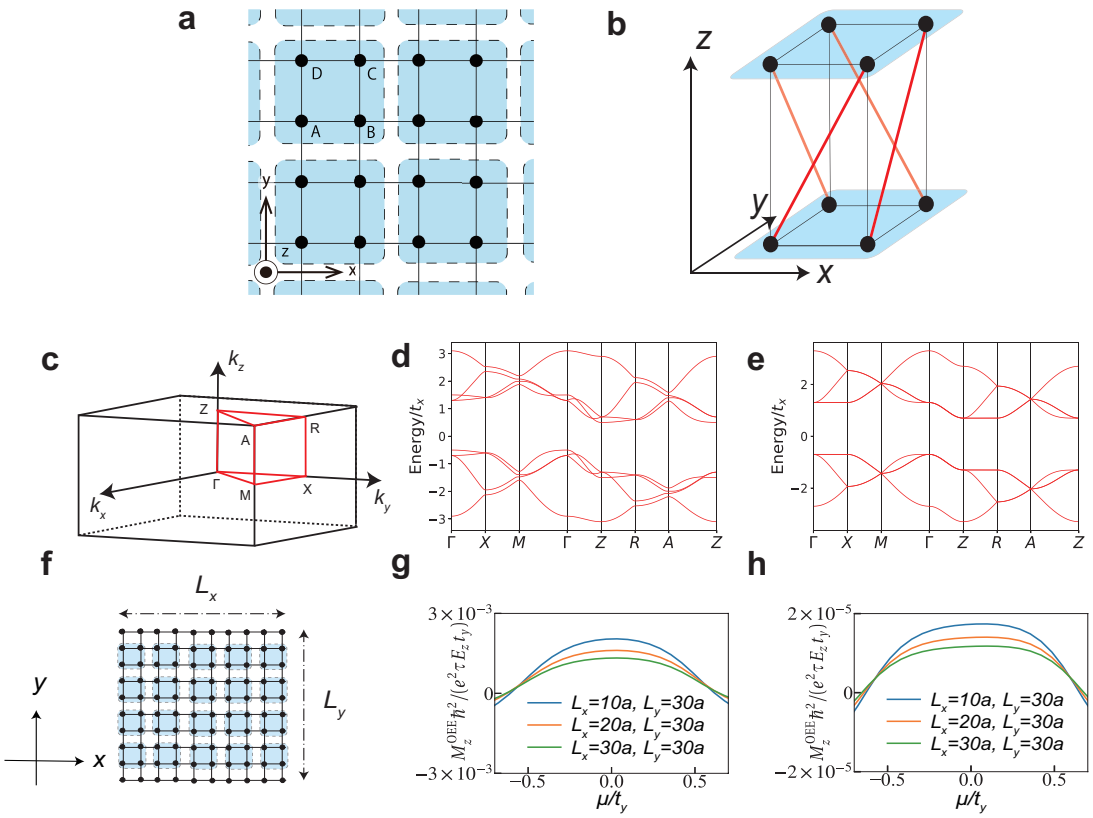

FIG. 1: **The model of a Chern insulator with a chiral structure and model calculation of the OEE.** (**a**) Individual layer of the model forming a square lattice. The blue regions surrounded by the broken line are the unit cells consist of four sublattices. (**b**) Schematic picture of the chiral hopping (red) between the two neighboring layers. These hoppings form structure similar to right-handed solenoids. (**c**) Brillouin zone of our model with high-symmetry points. (**d, e**) Energy bands for the Hamiltonian H with parameters (**d**) $t_x = t_y = m = b_x = b_y$, $t_3 = 0.1t_y$ and $t_4 = 0.15t_y$ and (**e**) $t_x = t_y = m = b_x = b_y$, $t_3 = 0.001t_y$ and $t_4 = 0.15t_y$. (**f**) One-dimensional model with periodic boundary condition in z direction. In order to see the boundary effect on OEE, the outermost layers on the xz surface has no chiral hoppings and those on the yz surface has chiral hoppings. (**g, h**) OEE calculated with parameters (**g**) $t_x = t_y = m = b_x = b_y$, $t_3 = 0.1t_y$ and $t_4 = 0.15t_y$ and (**h**) $t_x = b_x = t_y$, $t_y = b_y = m$, $t_4 = 0.15t_y$, and $t_3 = 0.001t_y$.

relaxation time assumed to be constant and $f^0(E)$ is the Fermi distribution function $f^0(E) = (e^{\beta(E-\mu)}+1)^{-1}$, $\beta = 1/k_BT$, k_B is the Boltzman constant and μ is the chemical potential. Then the orbital magnetization is generated as

$$M_z^{\rm OEE} = \frac{1}{2\pi}\int_{-\pi/c}^{\pi/c} dk_z \frac{1}{S}\sum_n^N \frac{e\tau E_z}{\hbar}\frac{\partial f^0(E_n(k_z))}{\partial k_z} \times\left(-\frac{e}{2}\right)\langle\psi_n(k_z)|(\mathbf{r}\times\mathbf{v})_z|\psi_n(k_z)\rangle. \quad (2)$$

This is the OEE. This calculation method is different from that in the previous study on metals[1,2,4], where bulk contribution in a system infinite along x and y directions are calculated.

Model calculation on a Chern insulator. As an example of a topological insulator, we consider an orbital magnetization in a Chern insulator with a chiral crystal structure. For this purpose, we introduce a three-dimensional tight-binding model of a layered Chern insulator, as shown in Fig. 1a, connected via right-handed interlayer chiral hoppings (Fig. 1b). Each layer forms a square lattice within the xy-plane, with a lattice constant a, and they are stacked along the z-axis with a spacing c. as shown in detail in Methods. The Brillouin zone and the band structure is shown in Figs. 1c-e. We set the Fermi energy in the energy gap.

We calculate OEE in a one-dimensional quadrangular prism with xz and yz surfaces shown in Fig. 1f (see Methods), with its results in Figs. 1g and 1h with the interlayer hopping $t_3 = 0.1t_y$ and $t_3 = 0.001t_y$, respectively, for several values of the system size, L_x and L_y, representing the lengths of the crystal in the x and y directions. Thus, the OEE is affected by boundaries and system size, and this size dependence remains even when the system size is much larger than the penetration depth of topological surface states. Therefore, OEE cannot be defined as a bulk quantity. Later, we give an interpretation on this characteristic size dependence.

Surface theory of OEE for a slab. In topological

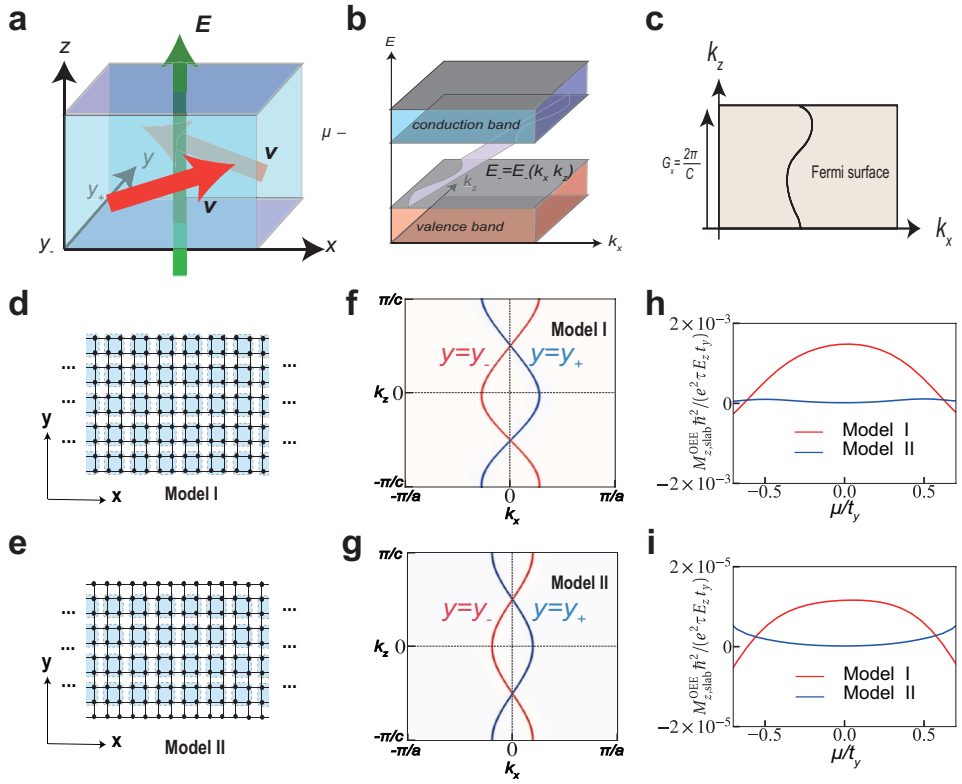

FIG. 2: **A Chern insulator with a chiral structure and OEE in slab systems.** (**a**) Surface velocity of the topological surface state under an electric field. (**b, c**) Band structure of the topological chiral surface states on the $y = y_-$ surface. Their (**b**) dispersion and (**c**) Fermi surface are shown. (**d**) Slab model I with chiral hopping on the surface. (**e**) Slab model II with no chiral hopping on the surface. (**f, g**) The fermi surfaces for the slab models (**f**) I and (**g**) II with parameters $t_x = t_y = m = b_x = b_y$, $t_3 = 0.1t_y$, $t_4 = 0.15t_y$ and $\mu = 0$. (**h, i**) OEE for the slab models I and II with parameters (**h**) $t_x = t_y = m = b_x = b_y$, $t_3 = 0.1t_y$ and $t_4 = 0.15t_y$ and (**i**) $t_x = t_y = m = b_x = b_y$, $t_3 = 0.001t_y$ and $t_4 = 0.15t_y$.

insulators such as Chern insulators, only the topological surface states can carry a current. Here we calculate the OEE using an effective Hamiltonian for the crystal surface. Thereby, we can capture natures of OEE through this surface theory. We consider slab systems, with its surfaces on $y = y_\pm$ ($y_+ > y_-$). The slab is sufficiently long along the x and z directions and we impose periodic boundary conditions in these directions. To induce the orbital magnetization $M^{\rm OEE}_{z,\rm slab}$, we apply an electric field E_z in the z direction. Due to the interlayer chiral hoppings, the surface current acquires a nonzero z-component (Fig. 2a).

Let $E_- = E_-(k_x, k_z)(= E_-(k_x, k_z + \frac{\pi}{c}))$ be the surface-state dispersion on the $y = y_-$ surface as shown in Fig. 2b and c. For simplicity, we assume C_{2z} symmetry of the system. Then the surface state dispersion on the $y = y_+$ surface is given by $E_+ = E_+(k_x, k_z) = E_-(-k_x, k_z)$. Here, we assume that the surface states are sharply localized at $y = y_\pm$, namely, we ignore finite-size effects due to a finite penetration depth. Then, we rewrite equation (2) to

$$M^{\rm OEE}_{z,\rm slab} = \frac{e^2\tau E_z}{2\hbar^2}\int_{-\pi/c}^{\pi/c}\frac{dk_z}{(2\pi)^2} \times \frac{\partial E(k'_x,k_z)}{\partial k_z}\mathrm{sgn}\left(\frac{\partial E(k'_x,k_z)}{\partial k'_x}\right)\Big|_{E(k'_x,k_z)=\mu}, \quad (3)$$

(see Supplementary Note 1 for details). We note that the Fermi surface depends on the surface termination, and so does the OEE. We also confirm the surface dependence from numerical calculations as shown in Figs. 2d-i. This formula applies to any topological insulators such as Z_2-TIs[40–42] (see Supplementary Note 2).

Surface theory of OEE for a cylinder. From this slab calculation, we calculate the OEE for a cylinder geometry. We consider a current along the z direction in a one-dimensional quadrangular prism with xz and yz surfaces (surfaces I-IV in Fig. 3) through its surface Hamiltonian. Let L_x and L_y denote the system sizes along the x and y directions, respectively. Because the OEE is sensitive to differences in crystal surfaces, as shown in slab systems, we consider the individual surfaces separately.

In particular, in Chern insulators we can calculate the energy eigenstates for the whole system from those for the

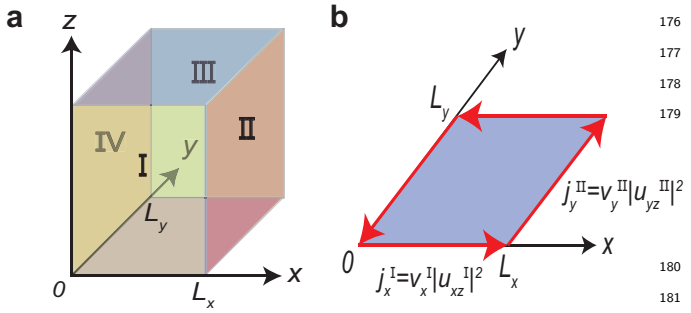

FIG. 3: **One-dimensional prism.** (**a**) Cross section of a one-dimensional system along xy-plane. (**b**) Current conservation at the corners.

surface Hamiltonians. For simplicity, we assume twofold rotation symmetry C_{2z} of the system, which relates between I and III, and between II and IV. Then, only the surface I and II are independent. We write down the eigenequations for these surfaces as

$$H^{\mathrm{I}}\psi^{\mathrm{I}}_{k_xk_z}(x,z) = E^{\mathrm{I}}_{k_xk_z}\psi^{\mathrm{I}}_{k_xk_z}(x,z), \quad (4)$$
$$H^{\mathrm{II}}\psi^{\mathrm{II}}_{k_yk_z}(y,z) = E^{\mathrm{II}}_{k_yk_z}\psi^{\mathrm{II}}_{k_yk_z}(y,z), \quad (5)$$

where H^{I} and H^{II} are the surface Hamiltonians for the surfaces I and II, respectively, and $\psi^{\mathrm{I}}_{k_xk_z} = u^{\mathrm{I}}_{k_xk_z}(k_x,k_z)e^{ik_xx}e^{ik_zz}$ and $\psi^{\mathrm{II}}_{k_yk_z} = u^{\mathrm{II}}_{k_yk_z}(k_y,k_z)e^{ik_yy}e^{ik_zz}$ are Bloch eigenstates on the surfaces I and II, respectively. We can determine these eigenstates from four conditions, equality of the energy eigenvalues, current conservation at the corner[43–45], periodic boundary condition on the crystal surface and the normalization condition (see Supplementary Note 3).

Thus we obtain a formula for OEE in a one-dimensional prism of a three-dimensional Chern insulator

$$M_z^{\mathrm{OEE}} = -\frac{e^2\tau E_z}{\hbar}\frac{1}{(2\pi)^2}\int_{-\pi/c}^{\pi/c}dk_z\frac{L_x\frac{\partial k_x^{\mathrm{I}}}{\partial k_z}+L_y\frac{\partial k_y^{\mathrm{II}}}{\partial k_z}}{\frac{L_x}{v_x^{\mathrm{I}}}+\frac{L_y}{v_y^{\mathrm{II}}}}\Big|_{E=\mu}, \quad (6)$$

where $v_x^{\mathrm{I}} = \frac{1}{\hbar}\frac{\partial E^{\mathrm{I}}}{\partial k_x}$ and $v_y^{\mathrm{II}} = \frac{1}{\hbar}\frac{\partial E^{\mathrm{II}}}{\partial k_y}$ and $k_x^{\mathrm{I}}(k_z,E)$ and $k_y^{\mathrm{II}}(k_z,E)$ are functions obtained from $E = E^{\mathrm{I}}_{k_xk_z}$ and $E = E^{\mathrm{II}}_{k_yk_z}$, respectively. When v_x and v_y are almost independent of k_z, we approximate equation (6):

$$M_z^{\mathrm{OEE}} = 2\frac{\frac{L_x}{\langle v_x^{\mathrm{I}}\rangle}M^{\mathrm{I,OEE}}_{z,\mathrm{slab}}+\frac{L_y}{\langle v_y^{\mathrm{II}}\rangle}M^{\mathrm{II,OEE}}_{z,\mathrm{slab}}}{\frac{L_x}{\langle v_x^{\mathrm{I}}\rangle}+\frac{L_y}{\langle v_y^{\mathrm{II}}\rangle}}, \quad (7)$$

where $M^{\mathrm{I,OEE}}_{z,\mathrm{slab}}$ and $M^{\mathrm{II,OEE}}_{z,\mathrm{slab}}$ represent the OEE for a slab (equation (3)) with the surface I and that with the surface II, respectively. Thus, the OEE of the one-dimensional system can be well approximated by equation (7) expressed in terms of that for the slabs along xz and along yz planes.

In general topological insulators, we can also derive OEE in terms of a simple picture of a combined circuit, consisting of four surfaces I- IV with anisotropic transport coefficients. We obtain

$$M_z^{\mathrm{OEE}} = j_{\mathrm{circ}} = \frac{\frac{L_x}{\sigma^{\mathrm{I}}_{xx}}\sigma^{\mathrm{I}}_{xz}+\frac{L_y}{\sigma^{\mathrm{II}}_{yy}}\sigma^{\mathrm{II}}_{yz}}{\frac{L_x}{\sigma^{\mathrm{I}}_{xx}}+\frac{L_y}{\sigma^{\mathrm{II}}_{yy}}}E_z, \quad (8)$$

where j_{circ} is the circulating current density within the xy plane around the prism per unit length along the z-direction. $\sigma^{\mathrm{I,II}}_{ij}$ is the electric conductivity tensor for the surfaces I and II (see Supplementary Note 4). On the other hand, we can also show $M^{\mathrm{I,OEE}}_{z,\mathrm{slab}} = \frac{1}{2}\sigma^{\mathrm{I}}_{xz}E_z, M^{\mathrm{II,OEE}}_{z,\mathrm{slab}} = \frac{1}{2}\sigma^{\mathrm{II}}_{yz}E_z$. In Chern insulators, by using $\sigma^{\mathrm{I}}_{xx} \propto \langle v_x\rangle$ and $\sigma^{\mathrm{II}}_{yy} \propto \langle v_y\rangle$, we arrive at equation (7). Thus, we can calculate the OEE from the surface electrical conductivity from equation (8), which depends on the aspect ratio L_x/L_y.

We numerically comfirm that the results of direct calculation by equation (2) and those for surface calculation by equation (7) agree well (Fig. 4a-c). When the interlayer hopping is large (Fig. 4c), they slightly deviate from each other. This is because we cannot ignore the k_z dependence of v_x and v_y and they are out of the scope of the approximate expression (7).

Finite-size effect. In our approximation theory, we assumed that the surface current is localized at the outermost sites and ignored a finite penetration depth. In fact, we can fit well the data with various system sizes with a trial fitting function which includes a finite-size effect in equation (7) (see Methods and Supplementary Note 5). From these results, the finite-size effect is of the order $1/L$ in the leading order, coming from the finite penetration depth. When the system size is much larger than the penetration depth, the result is well described by the surface theory as shown in Fig. 4d.

Material. Topological insulators without inversion symmetry can be a good platform for obtaining large OEE, because the current flows on the surface. Therefore, the closed loop created by the current is macroscopic and it efficiently induces the orbital magnetization, in contrast to the conventional OEE in metals, where sizes of current loops are microscopic. Moreover, the surface states of topological materials are robust against perturbations caused by impurities.

Under the non-inversion-symmetry constraint, we cannot diagnose Z_2-TIs easily because the Z_2 topological invariant is expressed in terms of k-space integrals. Our idea here is to use S_4 symmetry to diagnose Z_2-TIs, where we only need to calculate wavefunctions at four momenta according to the symmetry-based indicator theories[46–48]. After searching in the topological material database[49], we notice that $Cu_2ZnSnSe_4$[50] with ***82*** and $CdGeAs_2$ with ***122*** are two ideal candidates of Z_2-TIs with a direct gap for obtaining a large OEE (see Supplementary Note 6 for details). In the following, we will use $Cu_2ZnSnSe_4$, which only has S_4 symmetry as shown in Fig. 5a, as an example to show the magnitude of the OEE with different surfaces and different surface terminations.

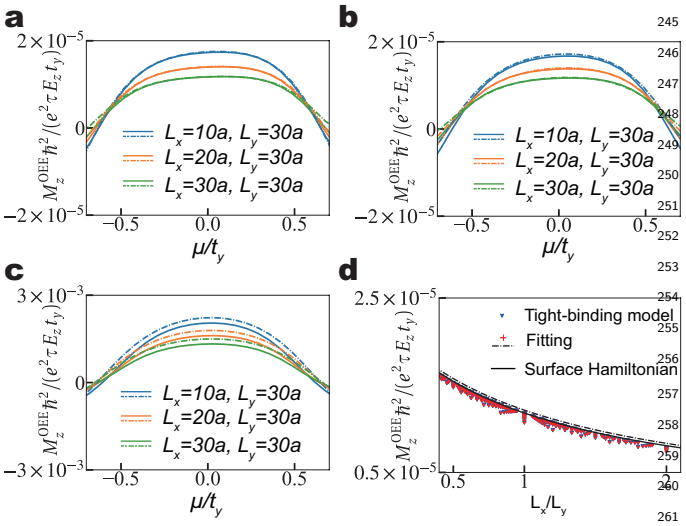

FIG. 4: **OEE in one-dimensional systems.** (**a-c**) OEE calculated from two different methods; one is a direct calculation by equation (2) (solid lines) and the other is by a combination of calculation results for surfaces along xz and yz planes based on equation (7) (dashed lines). Parameter values are (**a**) $t_x = t_y = m = b_x = b_y$, $t_3 = 0.001t_y$ and $t_4 = 0.15t_y$, (**b**) $t_x = b_x = 1.1t_y$, $t_y = b_y = m$, $t_4 = 0.15t_y$ and $t_3 = 0.001t_y$ and (**c**) $t_x = t_y = m = b_x = b_y$, $t_4 = 0.15t_y$ and $t_3 = 0.1t_y$. (**d**) Dependence on the aspect ratio within the xy plane with parameters $t_x = b_x = 1.1t_y$, $t_y = b_y = m$, $t_4 = 0.15t_y$, $t_3 = 0.001t_y$ and $\mu = 0$. Blue points represent the result of equation (2) for various system sizes. With parameter values $t_x = b_x = 1.1t_y$, $t_y = b_y = m$, $t_4 = 0.15t_y$, $t_3 = 0.001t_y$ and $\mu = 0$, we calculate the OEE with various system sizes from equation (2). The system sizes are $(L_x, L_y) \in \{10a, 12a, \ldots, 38a\} \times \{10a, 12a, \ldots, 38a\}$. Red points represent the result of fitting the numerical results of equation (2) with the fitting function equation (13), and its limit for L_x, $L_y \to \infty$ is shown as the dashed line. The solid line represent the results of equation (7).

Since the magnetoelectric tensor for the space group ***82***, defined by $\boldsymbol{M} = \boldsymbol{\alpha}\boldsymbol{E}$, is $\alpha_{\boldsymbol{82}} = \begin{bmatrix} \alpha_{11} & \alpha_{12} & 0 \\ \alpha_{12} & -\alpha_{11} & 0 \\ 0 & 0 & 0 \end{bmatrix}$, we can obtain an orbital magnetization M_1^{OEE} by adding an external electric field E_1, through the surface currents both on the [001] surface and on the [010] surface thanks to the nonzero α_{11} (see Supplementary Note 7 for details).

Figure 5c is the band structure of $Cu_2ZnSnSe_4$ with gap, through the first-principle calculations whose details are explained in Methods. On the [001] surface, terminations with Cu-Sn layer (surface A) and with Se layer (surface B) have different surface energies and Fermi surfaces, as shown in Fig. 5d-g, which contribute to a magnetoelectric susceptibility of $\alpha_{11}^{\mathrm{A}} = -1.804 \times 10^8 s^{-1}\Omega^{-1} \cdot\tau$ and $\alpha_{11}^{\mathrm{B}} = -2.565 \times 10^9 s^{-1}\Omega^{-1} \cdot\tau$, respectively. On the A surface, there is a single surface Dirac cone at Γ point, forming an electron-like Fermi surface. On the B surface, the Dirac cone at Γ point forms an almost zero Fermi surface, but two surface Dirac cones at two $\bar{X}$ momenta form two hole-like Femi surfaces. Because the Fermi surfaces on the B surface are much larger than those on the A surface, the magnetoelectric susceptibility on the B surface is one order of magnitude larger than that on the A surface. Similar calculations on the [010] surface are in the Supplementary Note 8, and the result is $\alpha_{11}^{\mathrm{C}} = -2.324 \times 10^9 s^{-1}\Omega^{-1} \cdot\tau$ for the surface C.

Let us compare the results with metallic materials in the bulk. For simplicity, we focus on the cases with the electric field $\boldsymbol{E}$ and the resulting magnetization $\boldsymbol{M}^{\mathrm{OEE}}$ along the z direction. This kinetic magnetoeletric response is expressed as $M_z^{\mathrm{OEE}} = \alpha_{zz}E_z$, and the conductivity is $j_z = \sigma_{zz}E_z$. Thus the magnetization in response to the current is $M_z^{\mathrm{OEE}} = (\alpha_{zz}/\sigma_{zz})j_z$. In the relaxation time approximation, both α_{zz} and σ_{zz} are proportional to the relaxatoin time τ. For simplicity we consider the system to be a cube with its size $L \times L \times L$. In the bulk metallic systems, the current is carried by the bulk states, and $\alpha_{zz} \propto L^0$, $\sigma_{zz} \propto L^0$. On the other hand, in topological systems, only the surface conducts the current, and the conductivity σ_{zz} scales as $\sigma_{zz} \propto L^{-1}$. On the other hand, we have shown $\alpha_{zz} \propto L^0$, which means that α_{zz} is an intensive quantity. Thus, in topological insulators, the scaling of the OEE as a response to the electric field is represented by the response coefficient $\alpha_{zz} \propto L^0$. Meanwhile, the response coefficient α_{zz}/σ_{zz} to the current is proportional to L. It means that as a response to the current, topological materials will generate a large amount of orbital magnetization as compared to metals.

We compare our results with OEE in p-doped tellurium, which has chiral crystal structure[5]. For the acceptor concentration $N_a = 4 \cdot 10^{14}\mathrm{cm}^{-3}$ at 50K, the induced orbital magnetizations is $M_z^{\mathrm{OEE}} = 7.0 \cdot 10^{-8}$ μ_{B}/atom $\sim 1.85 \times 10^{-2}$A/m by a current density $j_z = 1000\mathrm{A/cm}^2$. Thus the response coefficient of the orbital magnetization M_z^{OEE} to the current density j_z is $\alpha_{zz}/\sigma_{zz} = 1.85 \times 10^{-9}$m. If we approximate σ_{zz} by $\sigma_{zz} \sim \frac{N_a e^2 \tau}{m}$ with the electronic charge e and mass m, we get $\alpha = 2.1 \times 10^4$ $\mathrm{s}^{-1}\Omega^{-1} \cdot\tau$. For other acceptor concentrations $N_a = 4 \cdot 10^{16}\mathrm{cm}^{-3}$ and $N_a = 1 \cdot 10^{18}\mathrm{cm}^{-3}$, one can similarly get $\alpha_{zz} = 2.1 \times 10^6$ $\mathrm{s}^{-1}\Omega^{-1} \cdot\tau$ and $\alpha_{zz} = 2.3 \times 10^7$ $\mathrm{s}^{-1}\Omega^{-1} \cdot\tau$. Thus, the size of α_{zz} for the topological insulator $Cu_2ZnSnSe_4$ is larger than that of Te by two to five orders of magnitude.

On the other hand, in topological insulators, the induced orbital magnetization as a response to the current becomes huge compared with metals. To show this, we consider a system with surfaces having anisotropic transport coefficients. $\sigma_{xz}/\sigma_{zz} = \tan\theta$, where θ describes an angle between the electric field along the z direction and the surface current density $\boldsymbol{j}^{\mathrm{surf}}$. For example, for the [001] surface of $Cu_2ZnSnSe_4$, we get $\sigma_{21}^{\mathrm{A}} = 2\alpha_{11}^{\mathrm{A}} = -3.6 \times 10^8 s^{-1}\Omega^{-1} \cdot\tau$, $\sigma_{11}^{\mathrm{A}} = 7.3 \times 10^8 s^{-1}\Omega^{-1} \cdot\tau$, $\sigma_{21}^{\mathrm{B}} = 2\alpha_{11}^{\mathrm{B}} = -5.1 \times 10^9 s^{-1}\Omega^{-1} \cdot\tau$, $\sigma_{11}^{\mathrm{B}} = 2.0 \times 10^{10} s^{-1}\Omega^{-1} \cdot\tau$,

which yield $\tan\theta^{\rm A} = -0.49$ and $\tan\theta^{\rm B} = -0.26$ by identifying $x = 2$ and $z = 1$. Then the total current along the z direction is $4Lj_z$ while the circulating current is $j_{\rm circ} = j_x^{\rm surf} = j_z^{\rm surf}\tan\theta$. Thus the magnetization response $M_z^{\rm OEE}$ to the current density $j_z(= 4Lj_z^{\rm surf}/L^2)$ is $M_z^{\rm OEE}/j = (j_{\rm circ}/j_z^{\rm surf})(L/4) = (L/4)\tan\theta$. Thus for the macroscopic system size, the response $M_z^{\rm OEE}/j_z$ is also of the macroscopic size, and it is many order of magnitude larger than that in tellurium, where $M_z^{\rm OEE}/j_z$ is evaluated to be $M_z^{\rm OEE}/j_z = 1.85\times10^{-9}$m.

Discussion

In summary, we propose OEE in topological insulators with chiral structure. This OEE is carried by surface current due to the asymmetric crystal structure of the surface. Therefore, the OEE is sensitive to surface terminations, and it cannot be defined as a bulk quantity. We derive a formula for the OEE as a surface quantity using the surface Hamiltonian, and show that it fits with numerical results.

In theoretical treatments, atomic orbitals can classify the orbital magnetization into intraatom and interatom contributions. Some atomic orbitals such as $p_x \pm ip_y$ have orbital angular momentum, which leads to corresponding intraatomic orbital magnetization. On the other hand, the hopping between atoms lead, to the interatomic orbital magnetization. In tight-binding models with atomic orbitals, they are separately calculated. For example, in Refs. 10 and 11, the intraatomic orbital magnetization is studied, while Refs. 1, 2, and 15 consider the interatomic contributions. In real mateirals, these two contributions are not separable, and in the *ab initio* calculation[5], their sum is calculated. In this paper, we found that in topological materials, the interatomic contribution is much larger due to the macroscopic current loop. We show that the response to the current in topological insulators is much larger than in matels.

Methods

Details of the first-principle calculations First-principle calculations of $Cu_2ZnSnSe_4$ are implemented in the Vienna *ab initio* simulation package (VASP)[51–53] with Perdew-Burke-Ernzerhof exchange correlation. A Γ-centered Monkhorst-Pack grid with 10×10×10 k-points and 460.8 eV for the cut-off energy of the plane wave basis set is used for the self-consistent calculation. Surface states and Fermi surfaces calculations are performed by the tight-binding model obtained by the maximally localized Wannier functions[54].

Details of the model Hamiltonian. We consider a Chern insulating system with a chiral crystal structure. The model is composed of infinite layers of the two-dimensional Wilson-Dirac model[55,56]. The lattice sites are expressed by (i, j, l), with i, j, l being integers, specifying the x, y and z-coordinates. At each lattice site, we consider two orbitals 1 and 2. Let $c_{i,j,l,\sigma}$ denote the annihilation operator of electrons at the (i, j, l)-site with orbital $\sigma(= 1, 2)$, and we write $c_{i,j,l} = (c_{i,j,l,1}, c_{i,j,l,2})^T$. The model Hamiltonian is $H = H_{\rm WD}(m, t_x, t_y, b_x, b_y) + H_{\rm interlayer}(t_3, t_4)$, where $H_{\rm WD}$ is an in-plane Wilson-Dirac Hamiltonian, and $H_{\rm interlayer}$ is an interlayer Hamiltonian representing a structure similar to right handed solenoids. The in-plane Wilson-Dirac Hamiltonian is

$$\begin{aligned}
H_{\rm WD} &= m\sum_{i,j,l} c^\dagger_{i,j,l}\sigma_z c_{i,j,l} \\
&-\frac{it_x}{2}\sum_{i,j,l}(c^\dagger_{i,j,l}\sigma_x c_{i+1,j,l} - H.c.) \\
&-\frac{it_y}{2}\sum_{i,j,l}(c^\dagger_{i,j,l}\sigma_y c_{i,j+1,l} - H.c.) \\
&+\frac{b_x}{2}\sum_{i,j,l}(c^\dagger_{i,j,l}\sigma_z c_{i+1,j,l} + H.c. - 2c^\dagger_{i,j,l}\sigma_z c_{i,j,l}) \\
&+\frac{b_y}{2}\sum_{i,j,l}(c^\dagger_{i,j,l}\sigma_z c_{i,j+1,l} + H.c. - 2c^\dagger_{i,j,l}\sigma_z c_{i,j,l}), \quad (9)
\end{aligned}$$

where H.c. stands for Hermitian conjugate of the preceding terms, † represents Hermitian conjugate, and m, t_x, t_y, b_x and b_y are real parameters. This Hamiltonian $H_{\rm WD}$ can be rewritten in the momentum space as

$$\begin{aligned}
\tilde{H}_{\rm WD}(\mathbf{k}) &= t_x\sin k_x a\sigma_x + t_y\sin k_y a\sigma_y \\
&+ (m - b_x(1-\cos k_x a) - b_y(1-\cos k_y a))\sigma_z, \quad (10)
\end{aligned}$$

where $\mathbf{k}$ is the Bloch wavenumber. An isotropic version of the two-dimensional Wilson-Dirac model with $b \equiv b_x = b_y$ and $t_x = t_y$ exhibits the Chern insulating phase when $0 < m/b < 2$ and $2 < m/b < 4$[56]. Next we add interlayer hoppings, including a direct hopping t_4 along the z-axis and a chiral hopping t_3, where t_3 and t_4 are real parameters. To describe the chiral hopping t_3, the lattice sites in the square lattice in each layer into groups of four sites, $(2i-1, 2j-1), (2i-1, 2j), (2i, 2j-1)$ and $(2i, 2j)$ where i and j are integers, and we introduce chiral hoppings between the groups on the neighboring layers. Then the total Hamiltonian for this model on a tetragonal lattice is given by

$$H = H_{\rm WD} + H_{\rm interlayer}, \quad (11)$$

where

$$\begin{aligned}
H_{\rm interlayer} &= t_3\sum_{i,j,l}(c^\dagger_{2i-1,2j-1,l}c_{2i,2j-1,l+1} + H.c.) \\
&+t_3\sum_{i,j,l}(c^\dagger_{2i,2j-1,l}c_{2i,2j,l+1} + H.c.) \\
&+t_3\sum_{i,j,l}(c^\dagger_{2i,2j,l}c_{2i-1,2j,l+1} + H.c.) \\
&+t_3\sum_{i,j,l}(c^\dagger_{2i-1,2j,l}c_{2i-1,2j-1,l+1} + H.c.) \\
&+t_4\sum_{i,j,l}(c^\dagger_{i,j,l}c_{i,j,l+1} + H.c.). \quad (12)
\end{aligned}$$

These hoppings in $H_{\rm interlayer}$ form structures similar to right-handed solenoids. When $H_{\rm WD}$ in the Chern insulator phase, even if $H_{\rm WD}$ is perturbed by $H_{\rm interlayer}$, the system remains in the Chern insulator with the Chern

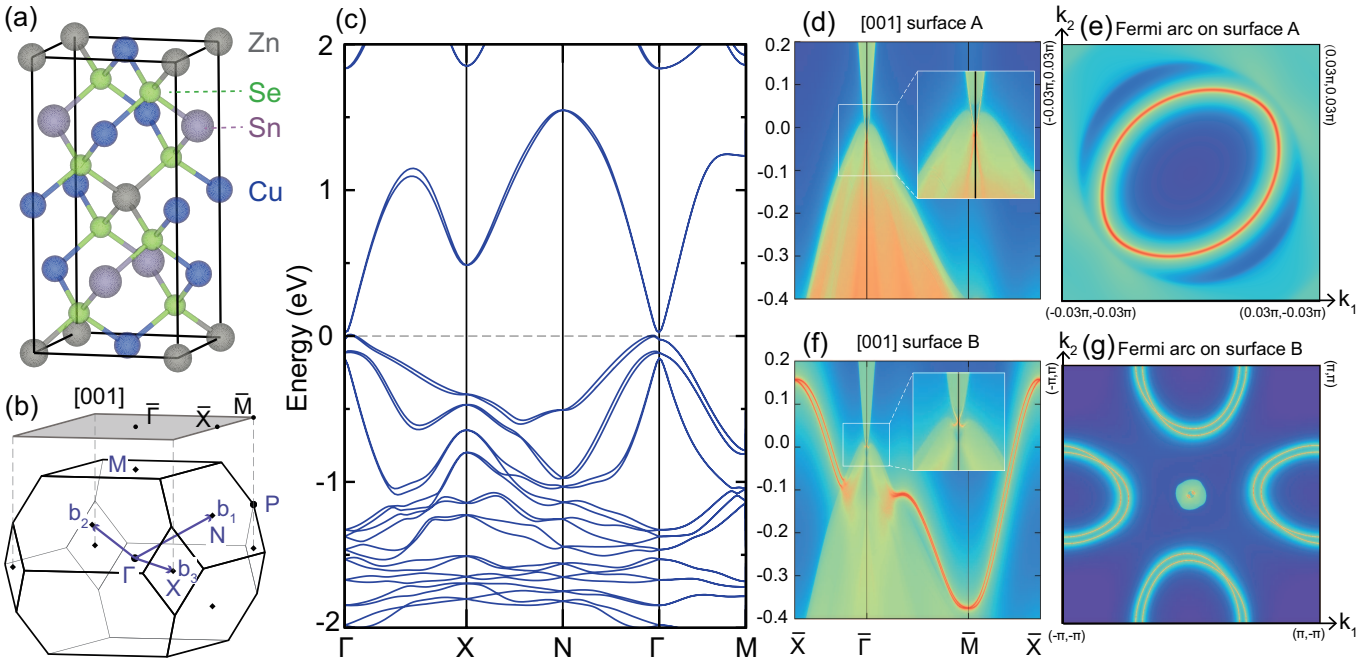

FIG. 5: **First principle calculations on $Cu_2ZnSnSe_4$.** (**a**) Crystal structure of $Cu_2ZnSnSe_4$. (**b**) Brillouin zone and surface Brillouin zone along [001] direction. (**c**) Electronic structure with spin-orbit coupling for the bulk. (**d-e**) Surface states and Fermi surface calculation on the [001] surface with Cu-Sn layer termination (surface A). (**f-g**) Surface states and Fermi arcs calculation on the [001] surface with Se layer termination (surface B).

number within the xy plane equal to -1 as long as t_3 and t_4 are small. In the main text, we are interested in the OEE due to the topological surface states in the topological Chern insulating phase, in which the Fermi energy is in the energy gap.

Fitting function for OEE. By taking into account the finite-size effect in equation (7), we give a fitting fuction. The finite penetration depth of the surface states will lead to $O(1/L)$ correction to the OEE, and that around the corner will lead to $O(1/L^2)$ correction[34]. Thus, the fitting function is

$$M_z^{\mathrm{OEE}} = \frac{w_1 L_x + w_2 L_y + w_3 + \frac{w_4}{L_x} + \frac{w_5}{L_y}}{w_6 L_x + w_7 L_y}, \qquad (13)$$

where $w_i (i = 1, 2, \ldots, 7)$ are real constants.

Acknowledgement

This work was supported by Japan Society for the Promotion of Science (JSPS) KAKENHI Grants No. JP18H03678, and No. JP20H04633, and by Elements strategy Initiative to Form Core Research Center (TIES), from MEXT Grant Number JP-MXP0112101001.

Additional information

The authors declare no competing financial interests.

Data availability statement

The datasets generated during and/or analysed during the current study are available from the corresponding authors on reasonable request.

Code availability statement

The source code for the calculations performed in this work is available from the corresponding authors upon reasonable request.

Author contribution

All authors contributed to the main contents of this work. K. O. performed the model calculation and formulated the theory for topological systems, through the discussions with T. Z. and S. M. T. Z. performed the *ab initio* calculation. S.M. conceived and supervised the project. All authors drafted the manuscript.

* murakami@stat.phys.titech.ac.jp

[1] T. Yoda, T. Yokoyama, and S. Murakami, Sci. Rep **5**, 12024 (2015).

[2] T. Yoda, T. Yokoyama, and S. Murakami, Nano Lett. **18**, 916 (2018).

[3] T. Furukawa, Y. Shimokawa, K. Kobayashi, and T. Itou, Nat. Commun. **8**, 954 (2017).

[4] S. Zhong, J. E. Moore, and I. Souza, Phys. Rev. Lett. **116**, 077201 (2016).

[5] S. S. Tsirkin, P. A. Puente, and I. Souza, Phys. Rev. B **97**, 035158 (2018).

[6] Y.-Q. Wang, T. Morimoto, and J. E. Moore, Phys. Rev. B **101**, 174419 (2020).

[7] J. E. Moore and J. Orenstein, Phys. Rev. Lett. **105**, 026805

(2010).
[8] I. Sodemann and L. Fu, Phys. Rev. Lett. **115**, 216806 (2015).
[9] Q. Ma, S.-Y. Xu, H. Shen, D. MacNeill, V. Fatemi, T.-R. Chang, A. M. M. Valdivia, S. Wu, Z. Du, C.-H. Hsu, S. Fang, Q. D. Gibson, K. Watanabe, T. Taniguchi, R. J. Cava, E. Kaxiras, H.-Z. Lu, H. Lin, L. Fu, N. Gedik, and P. Jarillo-Herrero, Nature **565**, 337 (2018).
[10] V. A. Shalygin, A. N. Sofronov, L. E. Vorob'ev, and I. I. Farbshtein, Physics of the Solid State **54**, 2362 (2012).
[11] T. Koretsune, R. Arita, and H. Aoki, Phys. Rev. B **86**, 125207 (2012).
[12] T. Furukawa, Y. Watanabe, N. Ogasawara, K. Kobayashi, and T. Itou, "Chirality-induced electrical generation of magnetism in nonmagnetic elemental tellurium," (2020), arXiv:2010.09210 [cond-mat.mtrl-sci].
[13] J. Rou, C. Şahin, J. Ma, and D. A. Pesin, Phys. Rev. B **96**, 035120 (2017).
[14] C. Şahin, J. Rou, J. Ma, and D. A. Pesin, Phys. Rev. B **97**, 205206 (2018).
[15] D. Hara, M. S. Bahramy, and S. Murakami, Phys. Rev. B **102**, 184404 (2020).
[16] W.-Y. He, D. Goldhaber-Gordon, and K. T. Law, Nat. Commun. **11**, 1650 (2020).
[17] V. Edelstein, Solid State Commun. **73**, 233 (1990).
[18] E. L. Ivchenko and G. E. Pikus, ZhETF Pisma Redaktsiiu **27**, 640 (1978).
[19] L. Levitov, Sov. Phys. JETP **61**, 133 (1985).
[20] R. Naaman and D. H. Waldeck, The Journal of Physical Chemistry Letters **3**, 2178 (2012).
[21] B. Gohler, V. Hamelbeck, T. Z. Markus, M. Kettner, G. F. Hanne, Z. Vager, R. Naaman, and H. Zacharias, Science **331**, 894 (2011).
[22] M. Kettner, V. V. Maslyuk, D. Nürenberg, J. Seibel, R. Gutierrez, G. Cuniberti, K.-H. Ernst, and H. Zacharias, The Journal of Physical Chemistry Letters **9**, 2025 (2018).
[23] B. P. Bloom, V. Kiran, V. Varade, R. Naaman, and D. H. Waldeck, Nano Letters **16**, 4583 (2016).
[24] O. B. Dor, N. Morali, S. Yochelis, L. T. Baczewski, and Y. Paltiel, Nano Letters **14**, 6042 (2014).
[25] T. Kimura, T. Goto, H. Shintani, K. Ishizaka, T. Arima, and Y. Tokura, Nature **426**, 55 (2003).
[26] H. Katsura, N. Nagaosa, and A. V. Balatsky, Phys. Rev. Lett. **95**, 057205 (2005).
[27] M. Fiebig, Journal of Physics D: Applied Physics **38**, R123 (2005).
[28] N. A. Spaldin and M. Fiebig, Science **309**, 391 (2005).
[29] F. Wilczek, Physical Review Letters **58**, 1799 (1987).
[30] A. M. Essin, J. E. Moore, and D. Vanderbilt, Phys. Rev. Lett. **102**, 146805 (2009).
[31] A. M. Essin, A. M. Turner, J. E. Moore, and D. Vanderbilt, Phys. Rev. B **81**, 205104 (2010).
[32] A. Malashevich, I. Souza, S. Coh, and D. Vanderbilt, New J. Phys. **12**, 053032 (2010).
[33] S. Coh, D. Vanderbilt, A. Malashevich, and I. Souza, Phys. Rev. B **83**, 085108 (2011).
[34] D. Ceresoli, T. Thonhauser, D. Vanderbilt, and R. Resta, Phys. Rev. B **74**, 024408 (2006).
[35] T. Thonhauser, D. Ceresoli, D. Vanderbilt, and R. Resta, Phys. Rev. Lett. **95**, 137205 (2005).
[36] D. Xiao, J. Shi, and Q. Niu, Phys. Rev. Lett. **95**, 137204 (2005).
[37] K.-T. Chen and P. A. Lee, Phys. Rev. B **86**, 195111 (2012).
[38] R. Bianco and R. Resta, Phys. Rev. Lett. **110**, 087202 (2013).
[39] A. Marrazzo and R. Resta, Phys. Rev. Lett. **116**, 137201 (2016).
[40] L. Fu, C. L. Kane, and E. J. Mele, Phys. Rev. Lett. **98**, 106803 (2007).
[41] J. E. Moore and L. Balents, Phys. Rev. B **75**, 121306(R) (2007).
[42] D. Hsieh, D. Qian, L. Wray, Y. Xia, Y. S. Hor, R. J. Cava, and M. Z. Hasan, Nature **452**, 970 (2008).
[43] A. Raoux, M. Polini, R. Asgari, A. R. Hamilton, R. Fazio, and A. H. MacDonald, Phys. Rev. B **81**, 073407 (2010).
[44] A. Concha and Z. Tešanović, Phys. Rev. B **82**, 033413 (2010).
[45] R. Takahashi and S. Murakami, Phys. Rev. Lett. **107**, 166805 (2011).
[46] H. C. Po, A. Vishwanath, and H. Watanabe, Nature communications **8**, 1 (2017).
[47] Z. Song, T. Zhang, Z. Fang, and C. Fang, Nature communications **9**, 1 (2018).
[48] E. Khalaf, H. C. Po, A. Vishwanath, and H. Watanabe, Physical Review X **8**, 031070 (2018).
[49] T. Zhang, Y. Jiang, Z. Song, H. Huang, Y. He, Z. Fang, H. Weng, and C. Fang, Nature **566**, 475 (2019).
[50] L. Guen, W. Glaunsinger, and A. Wold, Mater. Res. Bull. **14**, 463 (1979).
[51] G. Kresse and J. Hafner, Phys. Rev. B **47**, 558 (1993).
[52] G. Kresse and J. Hafner, Phys. Rev. B **49**, 14251 (1994).
[53] G. Kresse and J. Furthmuller, Comput. Mater. Sci. **6**, 15 (1996).
[54] A. A. Mostofi, J. R. Yates, Y.-S. Lee, I. Souza, D. Vanderbilt, and N. Marzari, Comput. Phys. Commun. **178**, 685 (2008).
[55] M. Creutz and I. Horváth, Phys Rev D **50**, 2297 (1994).
[56] Y. Yoshimura, K.-I. Imura, T. Fukui, and Y. Hatsugai, Phys. Rev. B **90**, 155443 (2014).

Figures

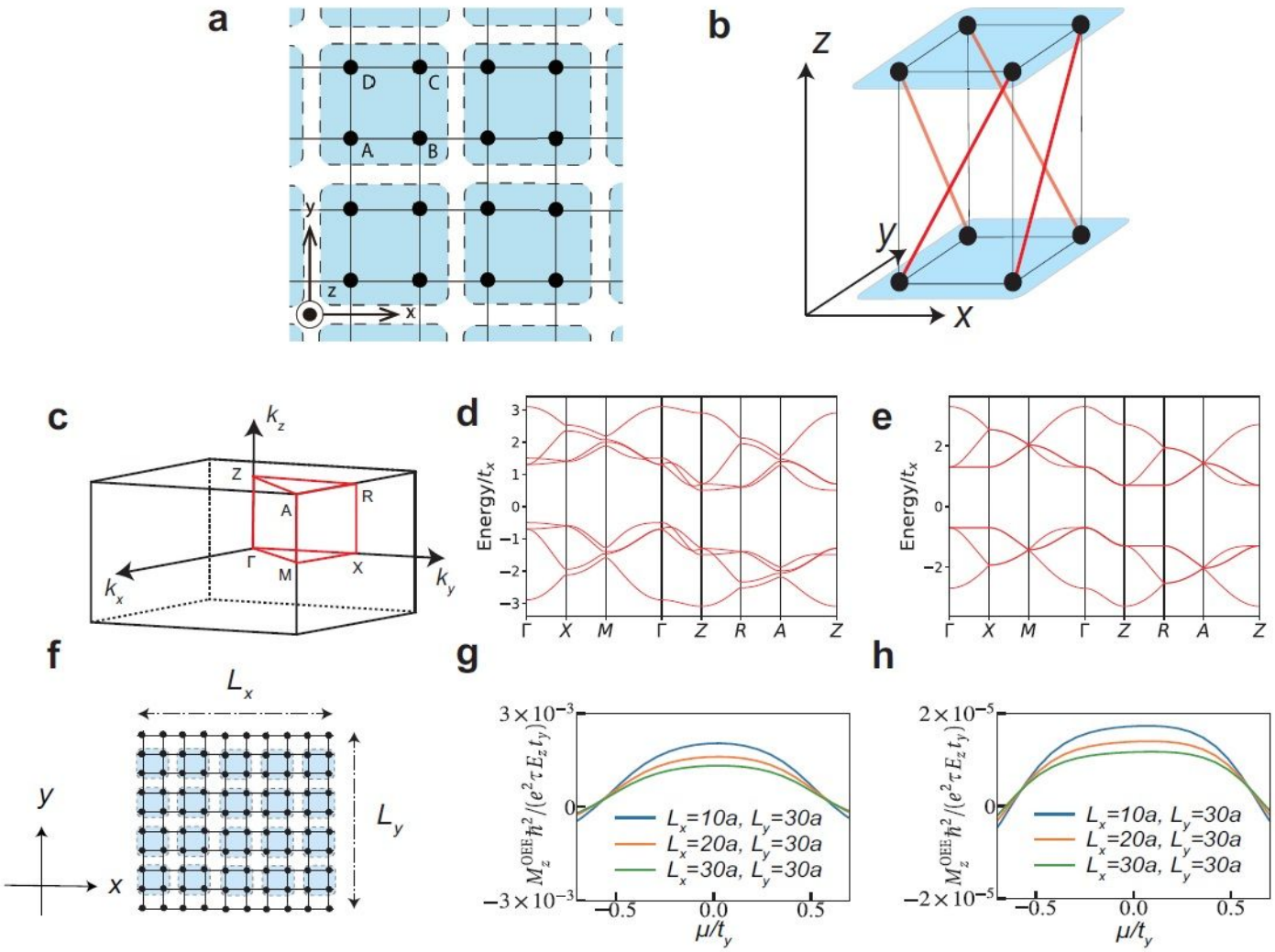

Figure 1

The model of a Chern insulator with a chiral structure and model calculation of the OEE. (a) Individual layer of the model forming a square lattice. The blue regions surrounded by the broken line are the unit cells consist of four sublattices. (b) Schematic picture of the chiral hopping (red) between the two neighboring layers. These hoppings form structure similar to right-handed solenoids. (c) Brillouin zone of our model with high-symmetry points. (d, e) Energy bands for the Hamiltonian H with parameters (d) tx = ty = m = bx = by, t3 = 0.1ty and t4 = 0.15ty and (e) tx = ty = m = bx = by, t3 = 0.001ty and t4 = 0.15ty. (f) One-dimensional model with periodic boundary condition in z direction. In order to see the boundary effect on OEE, the outermost layers on the xz surface has no chiral hoppings and those on the yz surface has chiral hoppings. (g, h) OEE calculated with parameters (g) tx = ty = m = bx = by, t3 = 0.1ty and t4 = 0.15ty and (h) tx = bx = ty, ty = by = m, t4 = 0.15ty, and t3 = 0.001ty.

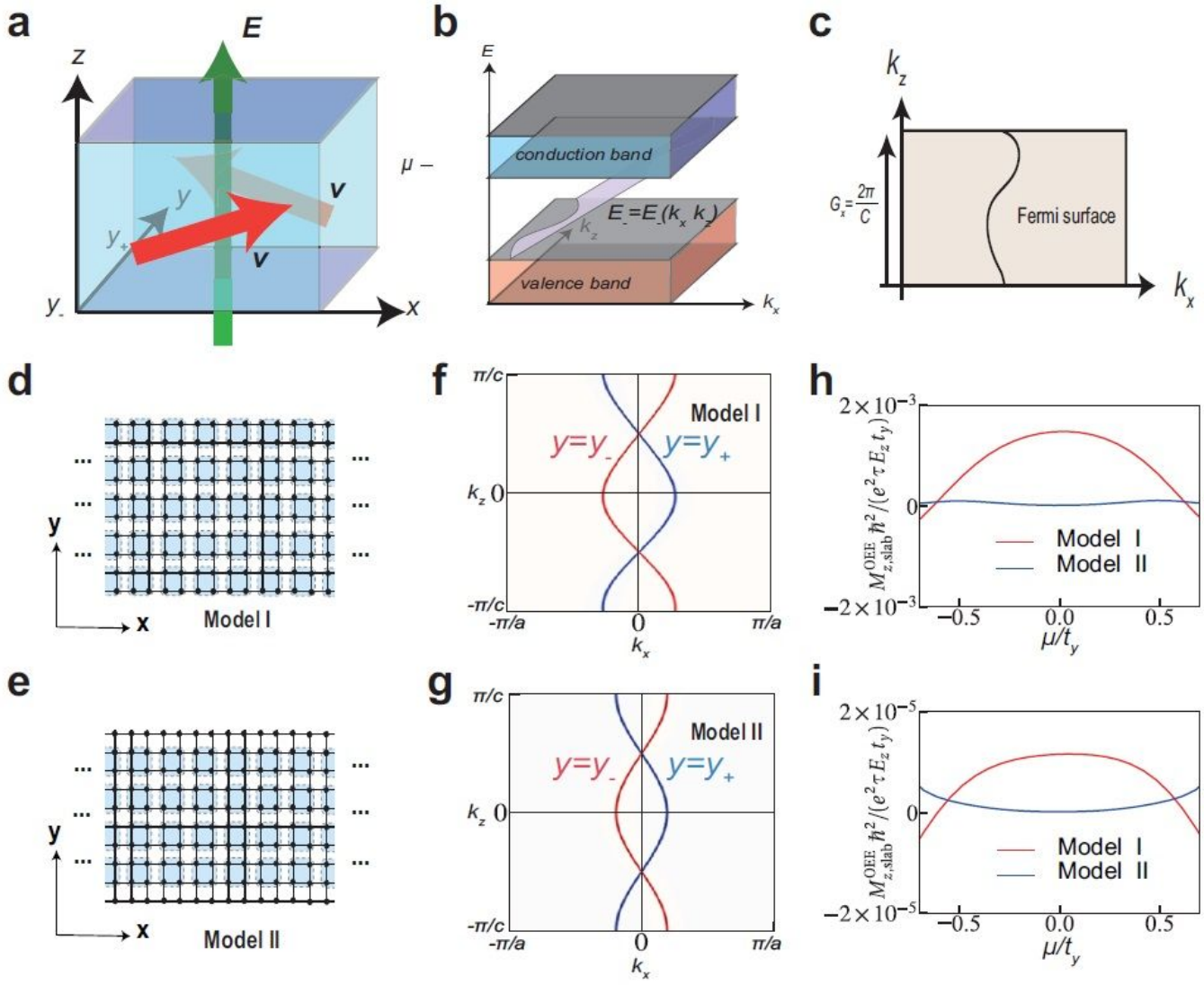

Figure 2

A Chern insulator with a chiral structure and OEE in slab systems. (a) Surface velocity of the topological surface state under an electric field. (b, c) Band structure of the topological chiral surface states on the y = y− surface. Their (b) dispersion and (c) Fermi surface are shown. (d) Slab model I with chiral hopping on the surface. (e) Slab model II with no chiral hopping on the surface. (f, g) The fermi surfaces for the slab models (f) I and (g) II with parameters tx = ty = m = bx = by, t3 = 0.1ty, t4 = 0.15ty and μ = 0. (h, i) OEE for the slab models I and II with parameters (h) tx = ty = m = bx = by, t3 = 0.1ty and t4 = 0.15ty and (i) tx = ty = m = bx = by, t3 = 0.001ty and t4 = 0.15ty.

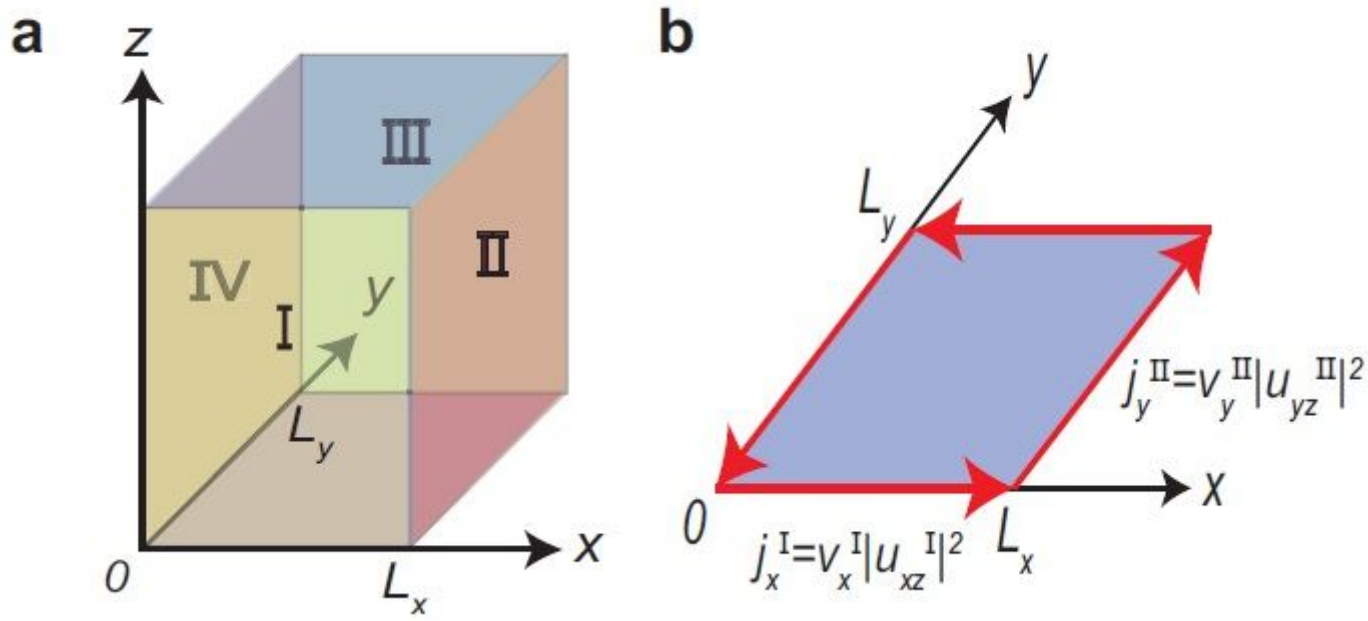

Figure 3

One-dimensional prism. (a) Cross section of a one-dimensional system along xy-plane. (b) Current conservation at the corners.

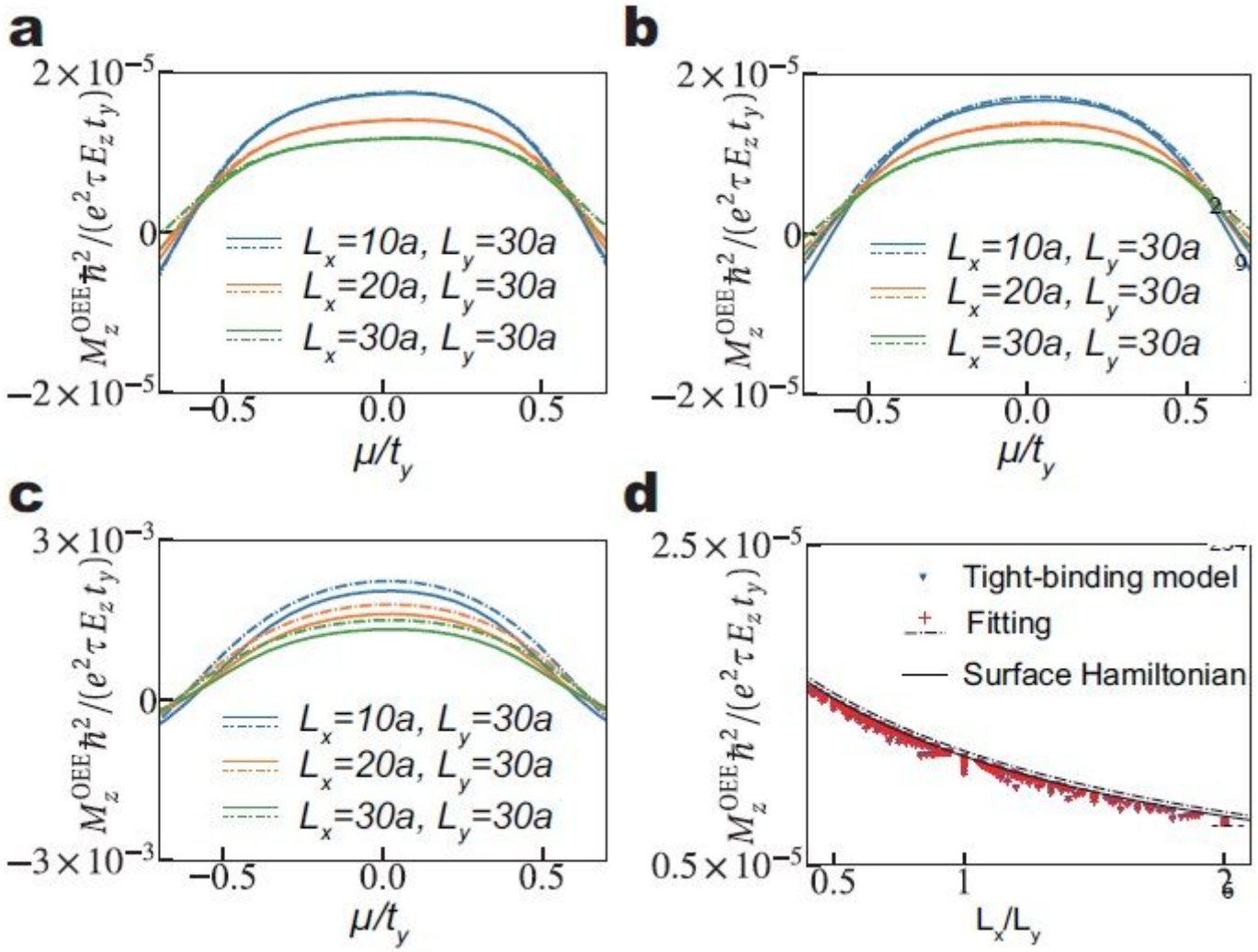

Figure 4

OEE in one-dimensional systems. (a-c) OEE calculated from two different methods; one is a direct calculation by equation (2) (solid lines) and the other is by a combination of calculation results for surfaces along xz and yz planes based on equation (7) (dashed lines).

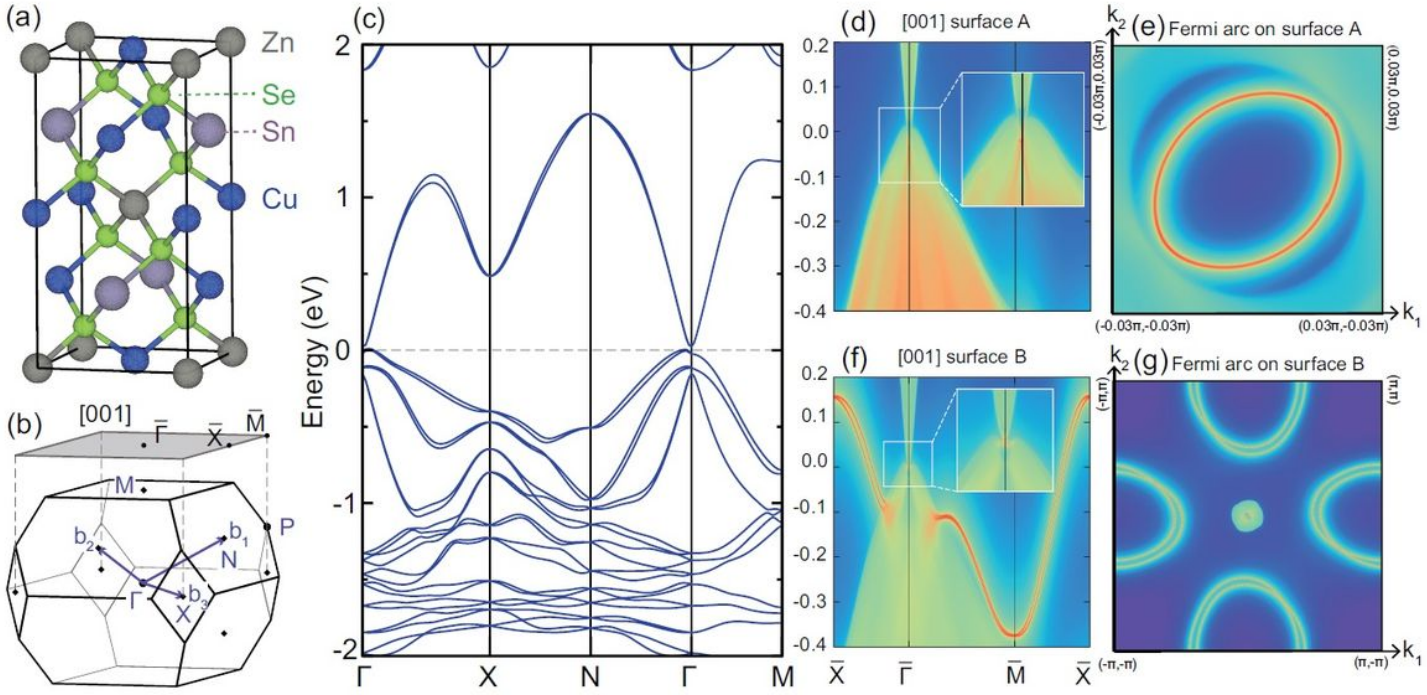

Figure 5

First principle calculations on Cu2ZnSnSe4. (a) Crystal structure of Cu2ZnSnSe4. (b) Brillouin zone and surface Brillouin zone along [001] direction. (c) Electronic structure with spin-orbit coupling for the bulk. (d-e) Surface states and Fermi surface calculation on the [001] surface with Cu-Sn layer termination (surface A). (f-g) Surface states and Fermi arcs calculation on the [001] surface with Se layer termination (surface B).

Supplementary Files

This is a list of supplementary files associated with this preprint. Click to download.

- SM210114a.pdf